Nutrition Research and Practice

Original Research

Check for updates

Centella asiatica extract prevents visual impairment by promoting the production of rhodopsin in the retina

Dae Won Park [2*], Hyelin Jeon [1,3*], Rina So [2], and Se Chan Kang [2,3§]

[1]Research Institute, Genencell Co. Ltd., Yongin 16950, Korea
[2]Department of Oriental Medicine Biotechnology, College of Life Sciences, Kyung Hee University, Yongin 17104, Korea
[3]BioMedical Research Institute, Kyung Hee University, Yongin 17104, Korea

OPEN ACCESS

§**Corresponding Author:**
Se Chan Kang
Department of Oriental Medicine Biotechnology, College of Life Sciences and BioMedical Research Institute, Kyung Hee University, 1732 Deogyeong-daero, Giheung-gu, Yongin 17104, Korea.
Tel. +82-31-201-5637
Fax. +82-31-201-8114
E-mail. sckang@khu.ac.kr

*These two authors contributed equally to this study.

ORCID iDs
Dae Won Park
https://orcid.org/0000-0003-4199-4446
Hyelin Jeon
https://orcid.org/0000-0001-9469-3677
Rina So
https://orcid.org/0000-0002-2113-3887
Se Chan Kang
https://orcid.org/0000-0003-0790-2237

ABSTRACT

BACKGROUND/OBJECTIVE: *Centella asiatica*, also known as Gotu kola, is a tropical medicinal plant native to Madagascar, Southeast Asia, and South Africa. It is well known to have biological activities, including wound healing, anti-inflammatory, antidiabetic, cytotoxic, and antioxidant effects. The purpose of this study was to determine the efficacy of extracts of *C. asiatica* against age-related eye degeneration and to examine their physiological activities.

MATERIALS/METHODS: To determine the effects of CA-HE50 (*C. asiatica* 50% EtOH extract) on retinal pigment cells, we assessed the cytotoxicity of $CoCl_2$ and oxidized-A2E in ARPE-19 cells and observed the protective effects of CA-HE50 against *N*-methyl-*N*-nitrosourea (MNU)-induced retinal damage in C57BL/6 mice. In particular, we measured factors related to apoptosis and anti-oxidation and the protein levels of rhodopsin/opsin. We also measured glucose uptake to characterize glucose metabolism, a major factor in cell protection.

RESULTS: Induction of cytotoxicity with $CoCl_2$ and oxidized-A2E inhibited decreases in the viability of ARPE-19 cells when CA-HE50 was administered, and promoted glucose uptake under normal conditions ($P < 0.05$). In addition, CA-HE50 inhibited degeneration/apoptosis of the retina in the context of MNU-induced toxicity ($P < 0.05$). In particular, CA-HE50 at 200 mg/kg inhibited the cleavage of pro-caspase-3 and pro-poly (ADP-ribose)-polymerase and maintained the expressions of nuclear factor erythroid 2-related factor 2 and heme oxygenase-1 similar to normal control levels. Rhodopsin/opsin expression was maintained at a higher level than in normal controls.

CONCLUSION: A series of experiments confirmed that CA-HE50 was effective for inhibiting or preventing age-related eye damage/degeneration. Based on these results, we believe it is worthwhile to develop drugs or functional foods related to age-related eye degeneration using CA-HE50.

Keywords: *Centella asiatica*; etinal degeneration; oxidative stress; cytoprotection

INTRODUCTION

Aging is a natural process, and aging-related diseases may be considered to be normal complications caused by aging. Aging leads to general decline in the functioning of the body and the development of diseases [1,2]. Among these, age-related eye diseases, including age-

Author Contributions

Conceptualization: Kang SC; Data curation: Park DW, Jeon H; Formal analysis: Park DW, So R; Funding acquisition: Kang SC; Investigation: Jeon H, So R; Methodology: Kang SC, Park DW; Project administration: Jeon H; Resources: Kang SC; Software: Park DW, So R; Supervision: Jeon H; Validation: Park DW, So R; Visualization: Park DW, Jeon H; Writing - original draft: Park DW, Jeon H; Writing - review & editing: Kang SC, Jeon H.

related macular degeneration, diabetic eye disease, and glaucoma, can affect quality of life [3]. Oxidative stress plays an important role in degenerative diseases associated with aging [2]. The retina is one of the most active tissues in the body and has high oxygen demand. In addition, the retina is particularly prone to the development of oxidative damage because it is constantly exposed to light and contains high concentrations of unsaturated fatty acids [4]. Treatment of oxidative stress of the retina requires longer-term sustainable management rather than a one-time treatment. Therefore, natural products with superior antioxidant and cytoprotective effects and significantly low toxicity are desired.

We examined *Centella asiatica* as a potential natural treatment to protect retinal cells from degeneration and apoptosis caused by oxidative stress. The main active ingredients of *C. asiatica* are saponins (triterpenoids), which include asiaticoside, asiatic acid, madecassoside, and madecassic acid [5]. In addition, plant sterols and flavonoids are present in the whole extract, in addition to tannins, essential acids, phytosterols, mucilages, resins, free amino acids, flavonoids, alkaloids, bitter components, and fatty acids that are known to have no pharmacological activity [6]. Known preclinical efficacy includes pharmacological effects such as wound healing [7], venous strengthening [8], cognitive enhancement [9], antioxidant and DNA damage preventive properties [10], epilepsy prevention [11], antiinflammatory effects [12], and antidepressant properties [13]. Based on these findings, we investigated the protective effects of *C. asiatica* extract in model systems including human retinal pigment epithelial cells and experimental animals in which we induced oxidative stress and cytotoxicity.

MATERIALS AND METHODS

Chemicals and reagents
All chemicals used in this work were purchased from commercial sources. All solvents were distilled via standard methods prior to use. Two compounds found in *C. asiatica* extract (asiatic acid [AA] and asiaticoside [AS]), 3-(4,5-dimethylathiazol-2-yl)-2,5-diphenyl-tetrazolium bromide (MTT), $CoCl_2$, *N*-retinylidene-*N*-retinylethanolamine (A2E), and lutein were purchased from Sigma-Aldrich (St. Louis, MO, USA). And *N*-methyl-*N*-nitrosourea (MNU) was purchased from Spectrum Chemical (New Brunswick, NJ, USA). Recombinant human insulin was obtained from ProSpec-Tany Technologene (Ness-Ziona, Israel).

Preparation of *Centella asiatica* extract
We produced extracts of *C. asiatica* using various % of EtOH solvents as follows. *C. asiatica* was collected from Jeju (Jeju-do, Korea) in August 2017 and positively identified by Professor Se Chan Kang, Kyung Hee University (Yongin, Gyeonggi-do, Korea). A voucher specimen (JBR536) was deposited in the Laboratory of Natural Medicine Resources in BioMedical Research Institute, Kyung Hee University. The samples were washed three times with distilled water to remove other plant materials and sand, dried without direct sunlight, and pulverized. The crude extract was obtained by extracting 2 kg of dried *C. asiatica* two times with 30%, 50%, and 70% EtOH for 24 h at room temperature. The extracts were concentrated for 16 h at reduced pressure and 40°C using a rotary evaporator, and then the extract was spray-dried to obtain powder and stored at −20°C before use. We referred to the *C. asiatica* 30%, 50%, and 70% EtOH extracts as CA30, CA50, and CA70, respectively. When used to treat cells, the extracts were mixed with autoclaved-distilled water. We used CA50, referred to as CA-HE50, as the final sample for all experiments described hereafter.

HPLC analysis

The HPLC analysis of CA-HE50 was conducted with an Agilent 1260 Infinity separation module coupled to a PDA detector, utilizing a Skypak C18 column 250 mm × 4.0 mm (particle size, 5 µm; SK chemicals, Seongnam, Gyeonggi-do, Korea) at a flow rate of 1.0 mL/min. The column was placed in a column oven at 40℃. The ratios of the mobile phases A (distilled water, Fisher Scientific Korea, Seoul, Korea) and B (acetonitrile, Fisher Scientific Korea) were changed after 0 (8:2, v/v), 35 (2:8, v/v), and 55 (8:2, v/v) minutes. The injection volume was 10 µL, and UV wavelength was 206 nm. Peaks were identified by comparing their retention times and UV-vis spectra with those of reference compounds. Detection of compound content in the CA-HE50 was performed using the external standard method, and AA and AS (ChemFaces, Wuhan, Hubei, China) were used as the standard stock solutions (12.5, 25, 50, and 100 µg/mL). Data were quantified using the corresponding cures of the reference compounds as standards.

Cell culture

ARPE-19, human retinal pigmented epithelium cells were obtained from American Type Culture Collection (ATCC, Manassas, VA, USA). ARPE-19 cells were cultured in Dulbecco's modified Eagle's medium/Nutrient Mixture F12 (DMEM/F12, Gibco, Grand Island, NY, USA) medium supplemented with inactivated 10% fetal bovine serum (FBS; Hyclone, South Logan, UT, USA) and 1% penicillin/streptomycin in a 37℃ incubator with a 5% CO_2 atmosphere.

Cell viability assay

ARPE-19 cells were seeded at a density of 3×10^4 cells/well in 96-well plates. After incubating overnight, the cells were treated with CA-HE50 and control samples (*C. asiatica* extracts and compounds) for 24 h. The cells were incubated with 10 µL of 5 mg/mL MTT (Sigma-Aldrich) for 4 h. After the supernatant was removed, 100 µL of dimethyl sulfoxide (DMSO) per well was added to the cells to dissolve the formazan crystals formed, and the cells were shaken twice for 4 to 5 sec. The optical density (OD) was measured at a 570 nm wavelength with a multi-reader (TECAN, Männedorf, Switzerland).

Protective effects of *C. asiatica* extracts and compounds against $CoCl_2$

To determine the IC_{50} of $CoCl_2$ against ARPE-19 cells, the concentration was adjusted to a maximum of 1 mM and incubated for 24 h. We then assessed the ARPE-19 cell protection effects of CA-HE50 and two compounds against 500 µM $CoCl_2$. After pretreatment with various concentrations of CA-HE50 for 2 h and then, we treated the cells with 500 µM of $CoCl_2$ for 24 h, and the subsequent treatment was performed in the same manner as the cell viability assay.

Protective effect of CA-HE50 against oxidized-A2E

We conducted this experiment to establish the conditions necessary for inducing the production of oxidized-A2E, which induces cytotoxicity. We diluted 100 µM of A2E in 0.5% DMSO-phosphate-buffered saline (PBS) and then irradiated the sample with UV (blue light, 430 nm) from 10 to 45 minutes, and then measured oxidized-A2E at 440 nm OD. We confirmed that more than half of the original 100 µM was oxidized after UV irradiation for 30 minutes. Therefore, these conditions were applied as experimental conditions. The test was designed to determine the effects of CA-HE50 on the production of oxidized A2E *in vitro*. CA-HE50 was added to empty 96-well plates at concentrations of 25, 50, and 100 µg/mL, and lutein 30 µg/mL was used as a positive control. After treating each well with 100 µM of A2E, the plates were UV irradiated for 30 minutes and the amount of oxidized A2E was measured. The OD was measured at a 440 nm wavelength with a multi-reader (TECAN). Finally, cell experiments were carried out as follows. ARPE-19 cells were seeded at a density of 3×10^4 cells/mL in 96-well

plates. After incubating overnight, the cells were treated with CA-HE50 and lutein for 2 h. After UV irradiation for 30 minutes, the survival rate of the cells was measured. The subsequent processes were performed in the same manner as the cell viability assays.

2-NBDG uptake assay

Glucose uptake activity was analyzed by measuring the uptake of 2-NBDG, a fluorescent D-glucose analogue. ARPE-19 cells were seeded on 96 well plates (1×10^4 cells/well) and cultured to 70% confluence in presence of FBS DMEM/F-12 media. Then, test substance CA-HE50 and insulin (positive control, 100 nM) were treated, respectively, and incubated for 24 h. After removing the media, we washed the cells twice with PBS warmed to 37°C and then added serum-free DMEM/F-12 media with 100 µM 2-NBDG and incubated the plates at 37°C in a 5% humidity chamber for 30 minutes. After washing twice with ice-cold PBS, the intracellular uptake of 2-NBDG was measured using a fluorimeter at excitation and emission wavelengths of 485 and 525 nm, respectively.

Animal care and experiments

Seven-week-old-male C57BL/6 mice were purchased from NARA Biotech (Seoul, Korea) and acclimated for 1 week before the experiment. Mice were housed in controlled environments of temperature (25 ± 3°C), humidity (53 ± 8%) under 12 h light/dark cycle, and ventilation of 10–12 times per hour. Animal experiments were performed in accordance with the current ethical regulations for animal care and use at Kyung Hee University (KHUASP(GC)-18-041). The mice weighed 21 ± 3 g and were randomly divided into five groups: normal control (NC); MNU (vehicle control); CA-HE50 in three concentrations and injected with MNU (MNU+CA-HE50). CA-HE50 doses were 50, 100, and 200 mg/kg. After an acclimation period, mice were provided with CA-HE50 dissolved in saline and administered orally for 7 days. MNU (Spectrum Chemical) dissolved in physiological saline containing 0.05% acetic acid was intraperitoneally administered at a concentration of 50 mg/kg, and mice were sacrificed 24 h later to collect blood and ocular samples.

Determination of liver tissue damage

After sacrifice, whole blood samples were harvested from the posterior vena cava and collected in EDTA-containing tubes. Serum was separated by centrifugation at 3,000 × g for 15 minutes at 4°C. Measurements of serum concentration of aspartate transaminase (AST) and alanine transaminase (ALT) were performed according to the manufacturer's instructions (Asan Pharm, Seoul, Korea). The parameters were analyzed using a multi-reader (TECAN).

H&E staining

At the time of sacrifice, eyeballs were harvested and fixed immediately in 4% paraformaldehyde (Sigma-Aldrich) for 4 h. The eye was dissected at the equator and the anterior eye and vitreous, including the lens, were removed. In order to prevent possible tissue damage during frozen section formation, they were left in 10% and 20% sucrose solution for 1 h and 30% sucrose solution for 12 h. After embedding in optical cutting temperature (OCT, SaKura Finetek, Torrance, CA, USA) solution, 4 µm thick tissue sections were prepared and stained with hematoxylin and eosin (H&E).

Western blot analysis

The left eye was separated using protein extraction solution (iNtRON, Seoul, Korea), and the obtained protein was quantified using a BCA protein assay kit (BIO-RAD, Hercules, CA, USA). Equal amounts of protein were mixed 1:1 with sample buffer (Laemmli sample buffer

(BIO-RAD) and 2-mercaptoethanol (BIO-RAD) mixed at 19:1) in each group and then heated at 99°C for 5 minutes. Heated protein was electrophoresed via 12% SDS polyacrylamide gel and transferred by electrophoretic means to nitrocellulose membrane. The membrane was blocked with 5% skim milk at room temperature, and then primary antibodies against the following proteins were used: rhodopsin (Abcam, Burlingame, CA, USA), opsin (Millipore, Burlington, MA, USA), heme oxygenase (HO-1, Cell Signaling, Beverly, MA, USA), nuclear enzyme erythroid 2-related factor-2 (NRF2, Santa Cruz Biotechnology, Santa Cruz, CA, USA), caspase 3 (Cell Signaling), and poly (ADP-ribose) polymerase (PARP, Cell Signaling). Horseradish-peroxidase-conjugated anti-mouse, and anti-rabbit secondary antibody were diluted in TBS-T solution. All western blots were re-probed with anti-β-actin antibody (Cell Signaling) to ensure protein loading. Bands were visualized with EZ-capture ST (ATTD) reagents according to the manufacturer's instructions.

Statistical analysis

Results are expressed as mean ± SEM for each experimental group. Statistical analysis was carried out using one-way analysis of variance followed by Tukey's test in SPSS 12.1K (IBM, Chicago, IL, USA). P-values less than 0.05 were regarded as significant.

RESULTS

Cytoprotective effects of *Centella asiatica* extract against CoCl$_2$

The cytoprotective effect of CA-HE50 was confirmed by inducing degeneration of ARPE-19 cell with excess cobalt. ARPE-19 cell cytotoxicity against CoCl$_2$ was confirmed by treatment with cobalt chloride for 24 h, up to 1000 μM concentration. The IC$_{50}$ of CoCl$_2$ for ARPE-19 cells was found to be 414.4 μM (**Fig. 1A**). Therefore, 500 μM, 24 h was set as the CoCl$_2$ treatment condition and the cytoprotective effect of *C. asiatica* extracts was confirmed. CA30 and CA50 were found to have cytoprotective effects against CoCl$_2$ at all concentrations (**Fig. 1B and C**), but unfortunately, no significant cytoprotective effect was found at any concentration for CA70 (**Fig. 1D**). The higher concentrations of CA extracts were expected to preserve cell viability. Unexpectedly, however, both CA30 and CA50 were associated with decreases in cell viability at the concentration of 100 μg/mL, and the cytoprotective effects of CA30 and CA50 showed similar trends, but the CA50 was associated with better protection. Therefore, we selected CA50 as the final material and refer to it as CA-HE50.

HPLC analysis of CA-HE50

AS and AA, known to exist in *C. asiatica*, were analyzed in CA-HE50. As shown in **Fig. 2**, the results of HPLC analysis of AS and AA revealed that 77.40 ± 19.92 mg/g and 5.23 ± 0.13 mg/g, respectively. We anticipated that both compounds would act as potents, and we used AS and AA in several subsequent experiments.

Cytoprotective effects of compounds present in CA-HE50

Like CA-HE50, we examined the cytotoxic effects of AA and AS in ARPE-19 cells and the cytoprotective effects against CoCl$_2$. We treated both components by two-fold serial dilution from 20 μg/mL to 0.625 μg/mL. Neither components were toxic to ARPE-19 cells. In particular, AA significantly increased cell viability at 20 μg/mL (**Fig. 3B**). The results of experiments with CoCl$_2$ are shown in **Fig. 3C and D**. As in the previous test, AA and AS were administered by concentration, respectively, and after 2 h, CoCl$_2$ was treated with 500 μM and left for 24 h. The cytoprotective effect on CoCl$_2$ was found to be significantly different from
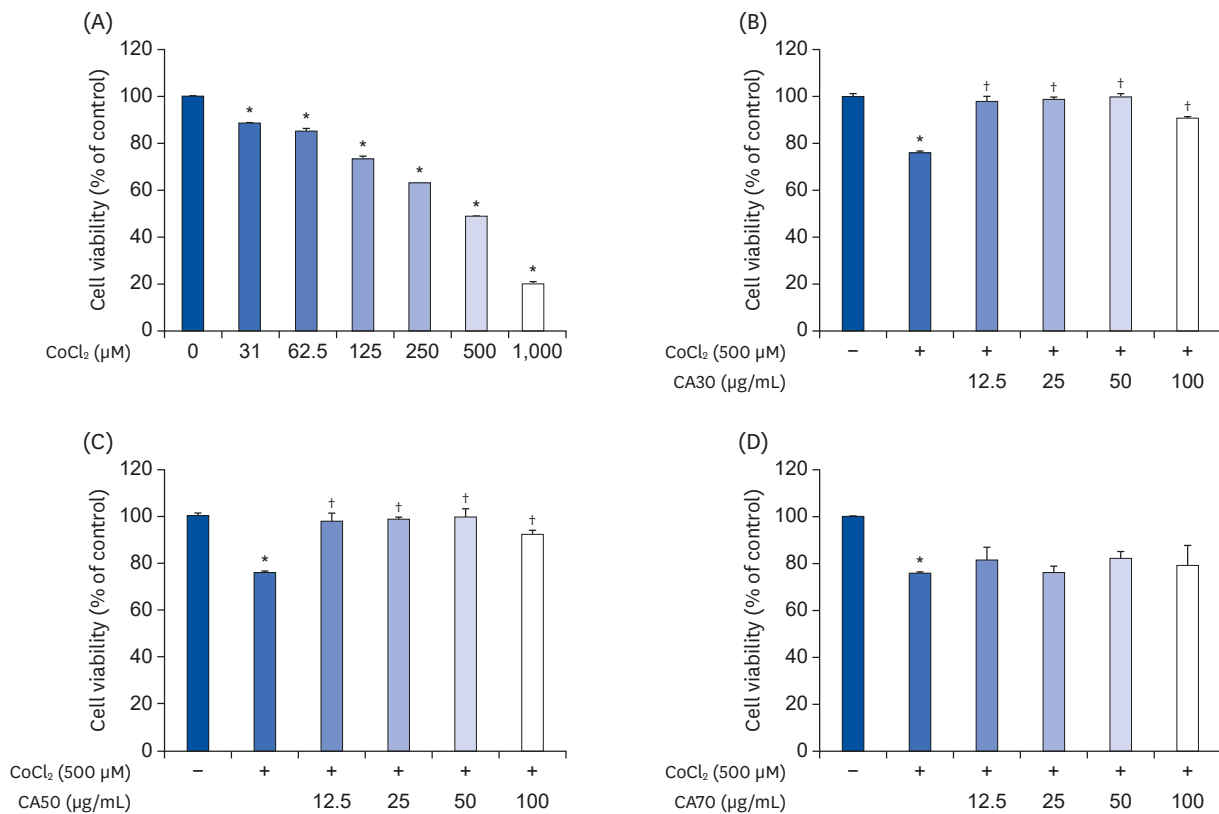
Fig. 1. Cytoprotective effects of CA-HE50 against $CoCl_2$ in ARPE-19 cells. (A) Cytotoxicity by $CoCl_2$ in ARPE-19 cells. Cytoprotective effects of (B) CA30, (C) CA50, and (D) CA70 against 500 μM $CoCl_2$. Representative data are expressed as mean ± standard error of the mean of three different experiments (n = 3) for each group.
*P < 0.05 compared with the normal control group. †P < 0.05 compared with the $CoCl_2$ control (vehicle) group.
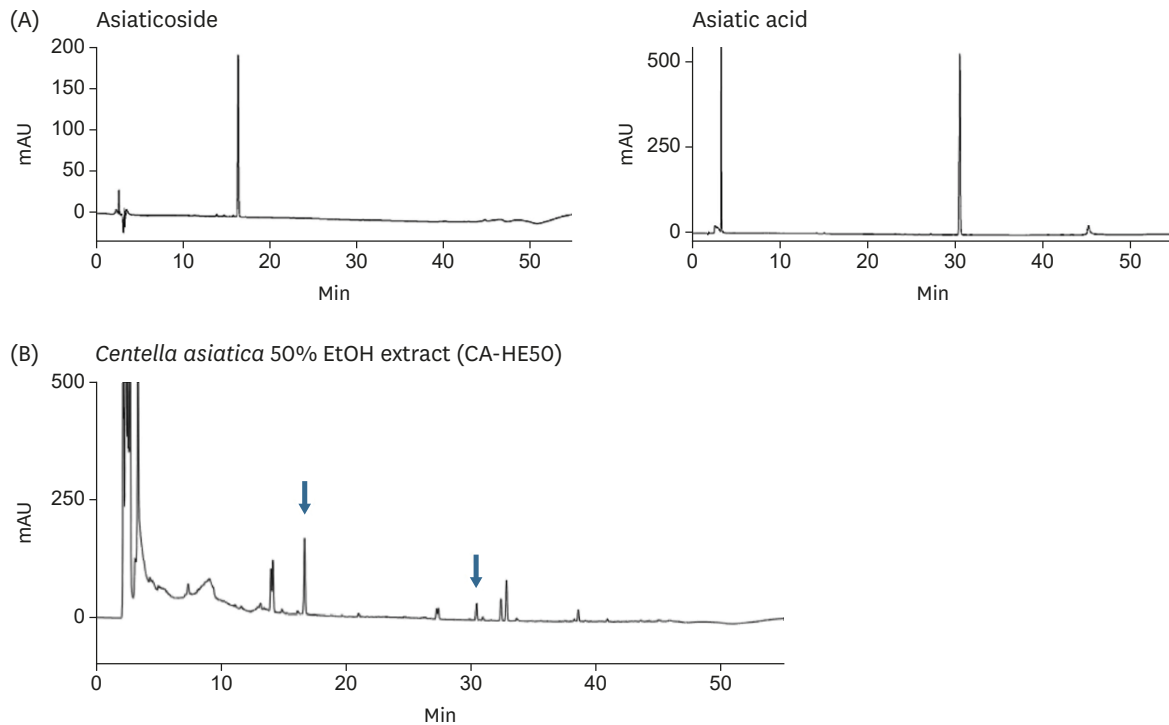

Fig. 2. High-performance liquid chromatography (HPLC-PDA) chromatograms of *C. asiatica* 50% EtOH extract (CA-HE50), asiaticoside, and asiatic acid. (A) HPLC chromatograms of asiaticoside and asiatic acid (standard). (B) HPLC chromatogram of CA-HE50.
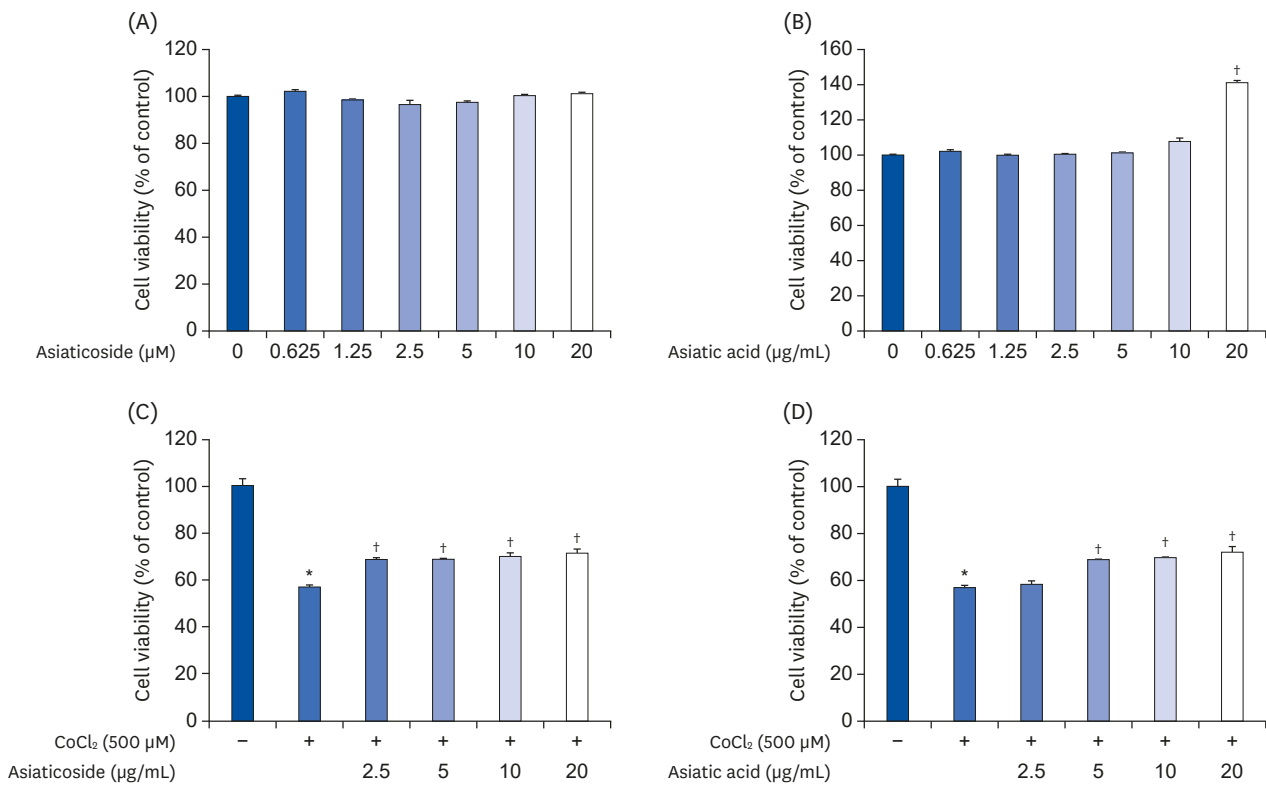
Fig. 3. Cytoprotective effects of asiaticoside and asiatic acid on $CoCl_2$ in ARPE-19 cells. Cytotoxicity of (A) AS and (B) AA in ARPE-19 cells. Cytoprotective effects of (C) AS and (D) AA on $CoCl_2$. Representative data are expressed as mean ± standard error of the mean of 3 different experiments (n = 3) for each group.
*$P < 0.05$ compared with the normal control group. †$P < 0.05$ compared with the $CoCl_2$ control (vehicle) group.

the concentration of 2.5 µg/mL in AS and 5 µg/mL in AA. Therefore, we determined that the cytoprotective effect of CA-HE50 is due to the presence of AS and AA.

Inhibitory effect of CA-HE50 on oxidized-A2E production

In another experiment, A2E was excessively treated to foster degeneration of ARPE-19 cells and photo-oxidation was induced by blue light. To determine the appropriate time for A2E to photo-oxidize, it was first tested *in vitro*. By dispensing 100 µM of A2E into a 96 well-plate and irradiating it with UV light over time, the amount of oxidized-A2E was confirmed. The production of oxidized-A2E was significantly increased after 10 minutes of UV irradiation. Therefore, 30 minutes, the time at which more than 50% was oxidized in 100 µM of A2E, was set as the test condition (**Fig. 4A**). Positive control lutein 30 µg/mL and CA-HE50 25, 50, and 100 µg/mL were dispensed into the test tube, then A2E 100 µM was added and UV irradiated for 30 minutes. As shown in **Fig. 4B**, we confirmed that the oxidation of A2E was suppressed in a concentration-dependent manner by CA-HE50 treatment. In particular, the production of oxidized-A2E was significantly inhibited at 50 and 100 µg/mL CA-HE50. After experimentally confirming that CA-HE50 may inhibit the production of oxidized-A2E *in vitro*, further experiments were carried out to determine the effects of CA-HE50 on the survival rate of ARPE-19 cells. As shown in **Fig. 4C**, when cells were treated with A2E and oxidized by UV, degeneration occurred in ARPE-19 cells and cell viability was reduced to 60% compared to normal control. On the other hand, when lutein and CA-HE50 were supplied, the cell survival rate was significantly increased compared to vehicle control. The cytoprotective effect of CA-HE50 against oxidative A2E was found to be concentrationdependent.
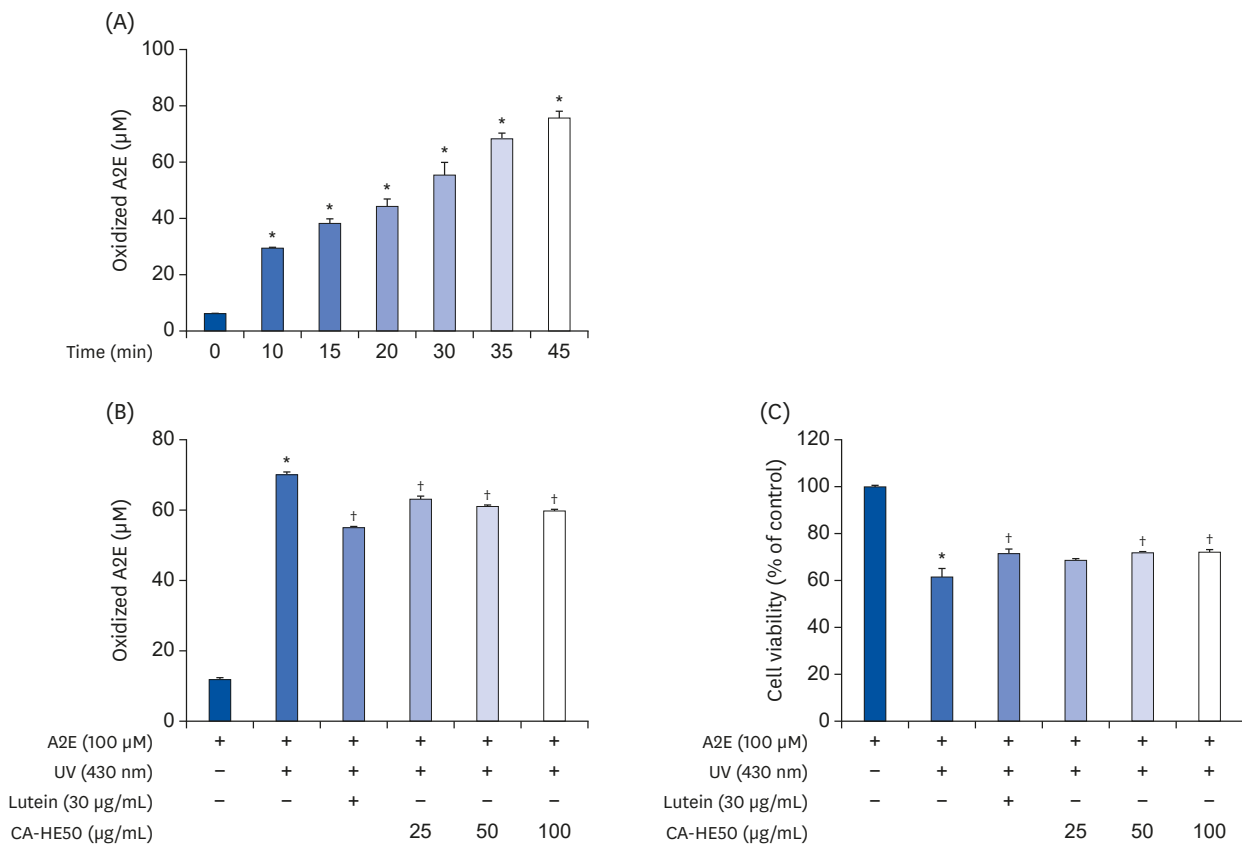
Fig. 4. Cytoprotective effects of CA-HE50 on oxidized-A2E in ARPE-19 cells. (A) Production of oxidized-A2E depends on UV-irradiation time. (B) Inhibitory effect of CA-HE50 on oxidized-A2E production. (C) Cytoprotective effect of CA-HE50 on oxidized-A2E in ARPE-19 cells. Representative data are expressed as mean ± standard error of the mean of three different experiments (n = 3) for each group.
A2E, a lipofuscin fluorophore; UV, ultraviolet.
*$P < 0.05$ compared with the normal control group. †$P < 0.05$ compared with the oxidized-A2E control (vehicle) group.

CA-HE50 helps transport glucose into retinal pigment cells

Several experiments were conducted to determine the cause of the cytoprotective effect of CA-HE50 on CoCl$_2$ and oxidized A2E. As shown in **Fig. 5**, we confirmed that glucose transport of ARPE-19 cells was increased by the presence of CA-HE50 and major components. At all tested concentrations, AS and AA resulted in significant differences in glucose transport. On the other hand, CA-HE50 showed a significant difference only at the concentration of 100 μg/mL. However, it showed a tendency to increase glucose transport in a concentration-dependent manner. In particular, significantly increased glucose transport was found at CA-HE50 100 μg/mL and AS and AA 5 μg/mL, an effect that was stronger than that of insulin, which was used as a positive control.

Protective effect of CA-HE50 in a model of *N*-methyl-*N*-nitrosourea-induced retina degeneration

MNU is as a pharmacological substance used to induce retinal degeneration in animal models [14]. Therefore, in animal experiments, we induced retinal damage with MNU to determine whether CA-HE50 has a protective effect against retinal damage. First, to determine the effects of MNU on overall animal health, we assessed blood ALT and AST. As shown in **Fig. 6**, MNU toxicity caused liver damage [15], resulting in AST and ALT levels that were more than double those of normal controls. However, CA-HE50 treatment resulted in a significant inhibition of liver damage due to its cytoprotective effects, similar to normal
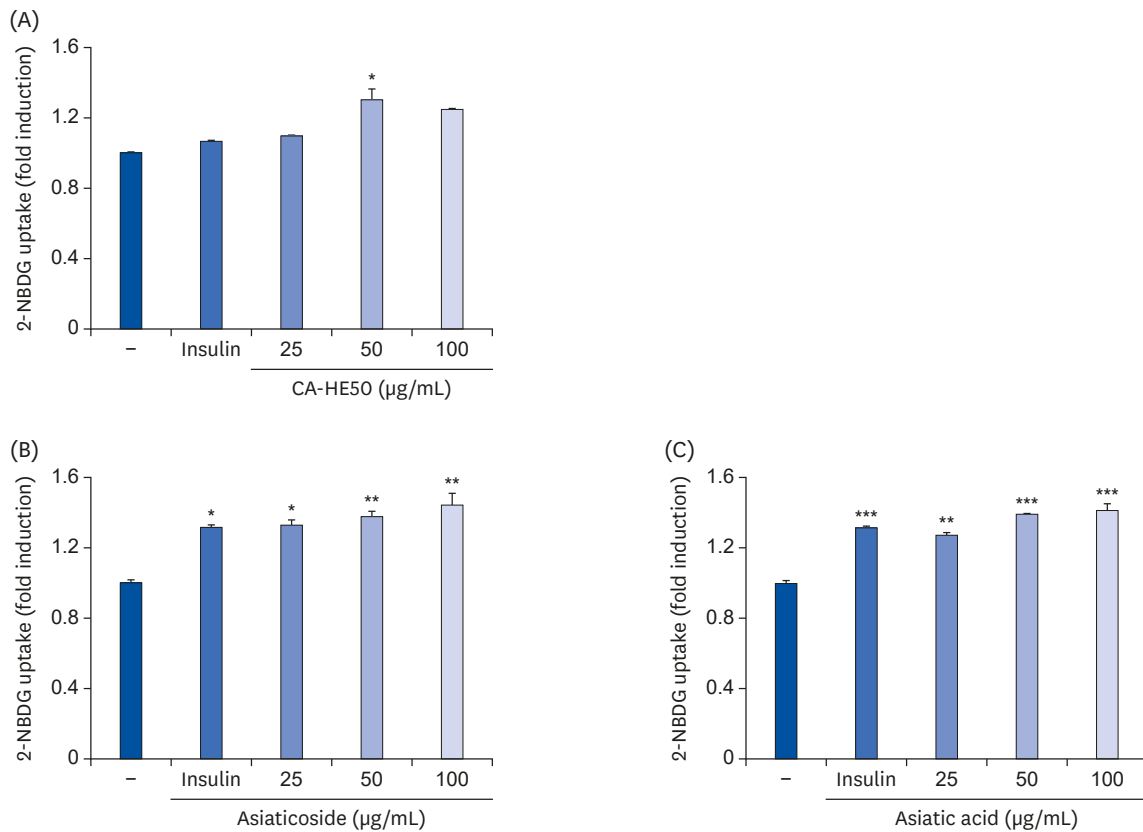
Fig. 5. Effects of CA-HE50, asiaticoside, and asiatic acid on glucose uptake in ARPE-19 cells. Effects of (A) CA-HE50, (B) AS, and (C) AA on glucose uptake in ARPE-19 cells. Representative data are expressed as mean ± standard error of the mean of 3 different experiments (n = 3) for each group.
*P < 0.05, **P < 0.01, and ***P< 0.001 compared with the control group.

control levels. The results of H&E staining of the eyeball were interpreted as follows. As shown in **Fig. 7**, when MNU was provided rather than normal control, the ONL disordered and RPE destruction was observed. On the other hand, when CA-HE50 was provided, we confirmed that ONL maintains a denser, more orderly arrangement than vehicle control, and at the same time, the arrangement of PRL was maintained evenly.
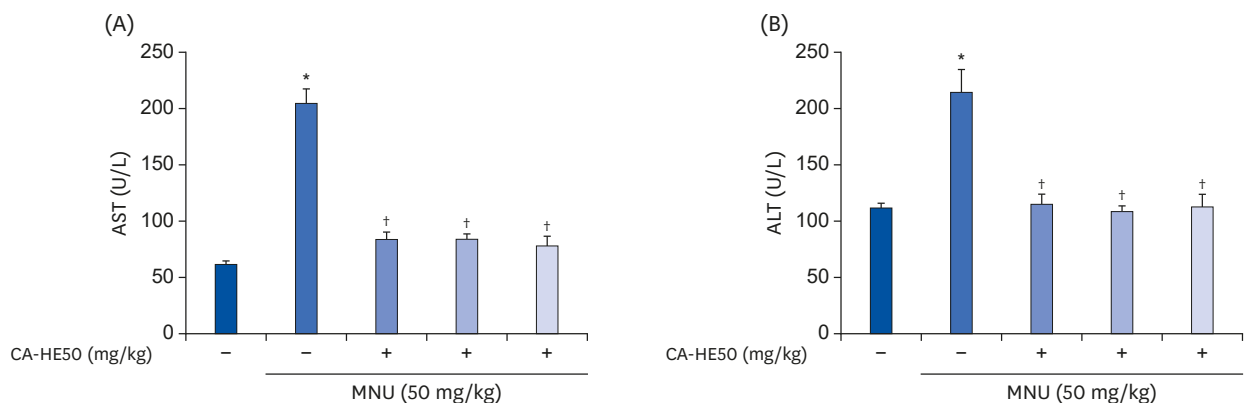

Fig. 6. Hepatoprotective effect of CA-HE50 against MNU-induced hepatotoxicity. (A) AST and (B) ALT release the inhibitory effect of CA-HE50. Representative data are expressed as mean ± standard error of the mean (n = 6) for each group.
MNU, *N*-methyl-*N*-nitrosourea; AST, aspartate aminotransferase; ALT, alanine aminotransferase.
*P < 0.001 compared with the normal control group. †P < 0.001 compared with the MNU (vehicle) control group.
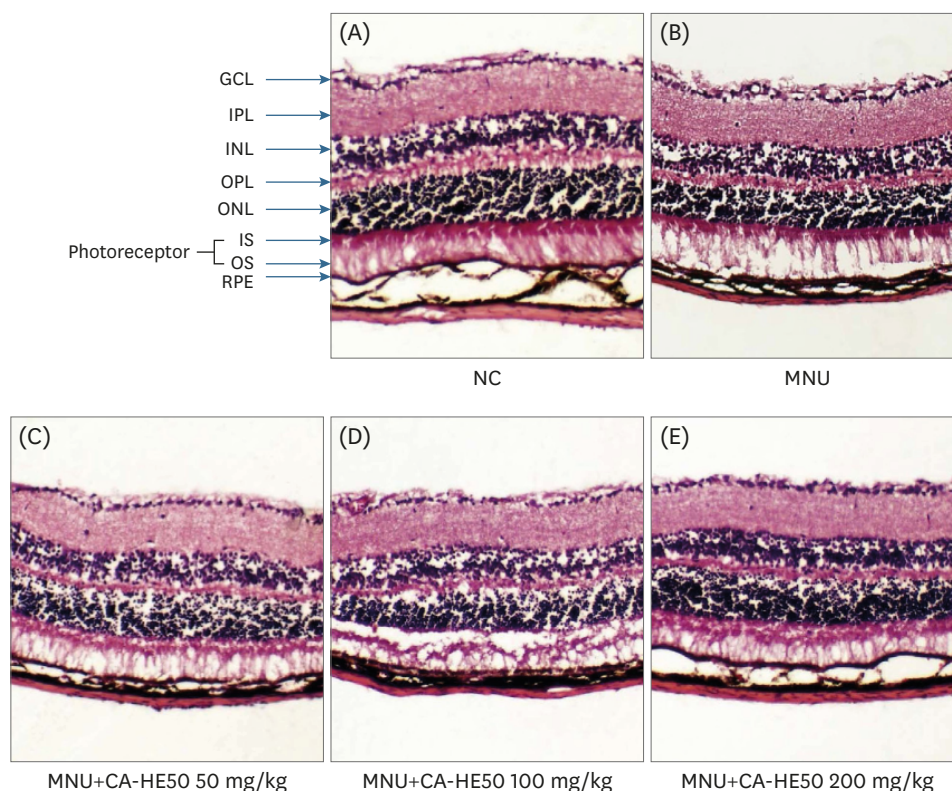
Fig. 7. Histopathology of retinas according to H&E staining from 5 groups of mice at 24 h post-injection. (A) Representative retinal images of H&E-stained retinal sections from normal (MNU-uninjected) eyes. (B) Representative retinal image from the MNU-injection group (vehicle group). (C) Representative retinal image for mice administered 50 mg/kg CA-HE50 for 7 days and then injected with MNU. (D) Representative retinal image for mice administered 100 mg/kg CA-HE50 for 7 days and then injected with MNU. (E) Representative retinal image for mice administered 200 mg/kg CA-HE50 for 7 days and then injected with MNU. Data are representative of 6 independent experiments.

MNU, *N*-methyl-*N*-nitrosourea; GCL, ganglion cell layer; IPL, inner plexiform layer; INL, inner nuclear layer; OPL, outer plexiform layer; ONL, outer nuclear layer; IS, inner segments; OS, outer segments; RPE, retinal pigment epithelium.

The mechanism underlying MNU-induced retinal degeneration is the induction of apoptosis in retinal photoreceptor cells [16]. Therefore, we examined the expression levels of apoptosis-related protein by MNU. As shown in **Fig. 8A**, the expressions of caspase-3 and PARP pro-forms associated with apoptosis were significantly reduced when MNU was given. On the other hand, when CA-HE50 was provided, the expressions of caspase-3 and PARP pro-forms increased significantly. The expression levels of NRF2 and HO-1 were significantly decreased in vehicle control, but in the CA-HE50 groups the expression was repaired. Based on these results, CA-HE50 was found to have antiapoptotic and anti-oxidation effects. In addition, we confirmed the presence of rhodopsin and opsin and their influence on visual acuity by western blotting analysis. When MNU was provided, the expression levels of rhodopsin and opsin were significantly lower than those of normal control (**Fig. 8B**). On the other hand, when CA-HE50 was orally administered, both rhodopsin and opsin expressions increased in a CA-HE50 concentration-dependent manner. In particular, when CA-HE50 200 mg/kg was provided, the expressions of rhodopsin and opsin were maintained at higher levels than normal control.

DISCUSSION

We sought to identify natural substances that could prevent or inhibit the development of RPE/photoreceptor degeneration in individuals with aging-related eye disease. We identified
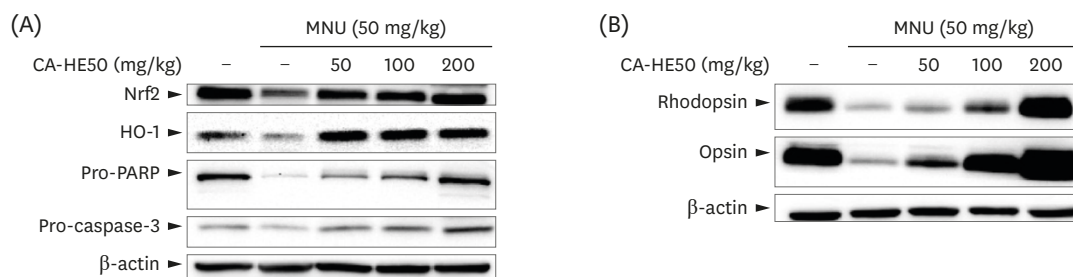
Fig. 8. Western blot analysis for expressions of proteins associated with retinal damage expressed in the eyes of C57BL/6 mice that induced retinal damage with MNU after 7 days of CA-HE50. (A) Effects of CA-HE50 on NRF2, HO-1, pro-PARP, and pro-caspase-3 at the protein level. (B) Effects of CA-HE50 on rhodopsin and opsin at the protein level. β-actin was detected as an internal standard. Data are representative of 6 independent experiments.
MNU, *N*-methyl-*N*-nitrosourea; NRF2, Nuclear factor erythroid 2-related factor 2; HO-1, heme oxygenase 1; PARP, Poly (ADP-ribose) polymerase.

natural materials that could be expected to have cytoprotective effects, and confirmed the protective effect of *C. asiatica* on ARPE-19 cells. Therefore, we obtained evidence that CA-HE50 is protective of the retinal pigment epithelial degeneration.

Cobalt is part of the vitamin B12 complex and is important for neuronal integrity [17]. However, excess cobalt induces hypoxia mimicry [18,19]. Tissue oxygenation and in particular hypoxia play important roles in retinal physiology and pathophysiology. Reduced oxygen tension and hypoxia-inducible transcription factors, along with some target genes, are critically involved in retinal development, especially in normal retinal vascular structures [20]. Therefore, timely hypoxia is essential for establishing proper retinal function and vision. However, increased oxygenation of the lens can reduce the clarity of the lens, which in turn can reduce the sensitivity of the visual system. In retinal pathology, hypoxia causes conditions of interest, such as high altitude-associated changes, retinopathy of prematurity, diabetic retinopathy, age-related macular degeneration, and glaucoma [21]. Therefore, cobalt chloride was used to induce hypoxia in cell experiments. Bioactive components are usually eluted well in organic solvents, so we prepared extracts with various concentrations of ethanol solutions (30, 50, and 70%). As described in the Results section, CA50 exhibited the best cytoprotective effects in ARPE-19 cells, and was therefore selected for a series of tests (**Fig. 1**). One of the factors causing age-related macular degeneration is lipofuscin (LF), which is a fluorescent complex mixture of highly oxidized and cross-linked macromolecules (proteins, lipids, and sugars) of varying metabolic origins [22,23]. Due to its polymer and highly cross-linked nature, LF is not degraded or cleaned by exocytosis. Therefore, LF accumulates in the lysosome and cell cytoplasm of aged animal cells [24,25]. In particular, exposure of spherical microparticles of LF to blue light in RPE contributes to atrophy in AMD patients by producing phototoxic and pro-inflammatory effects due to the mediation of reactive oxygen intermediates [26]. The main component, known as the fluorophore of LF, is bis-retinoid A2E, which is produced after metabolism in cells. It accumulates without being released from retinal pigment epithelial cells and is converted into its oxidized form by exposure to light stimulation or oxidative stress. Oxidized-A2E is known to induce retinal pigment epithelial and related photoreceptor degeneration [27,28]. For this reason, A2E was oxidized with blue light and experiments were conducted to confirm the cytoprotective effect of CA-HE50. CA-HE50 was found to inhibit the production of oxidized-A2E in a concentration-dependent manner and to inhibit the cytotoxicity of ARPE-19 cells. Thus, the cytoprotective effect of CA-HE50 in cytotoxic environments caused by $CoCl_2$ and oxidized-A2E was verified. These results suggest that CA-HE50 inhibits age-related RPE degeneration (**Fig. 4**).

Animal experiments were conducted to determine whether CA-HE50 inhibits age-related eye degeneration in vivo. Mammal eyes are very sensitive to toxic substances. Alkylating agents targeting photoreceptor cells such as MNU rapidly induce retinal damage through apoptosis in many animal species, including mice [29,30]. Such damage usually develops into benign and malignant tumors several months after exposure to MNU and rapidly causes specific photoreceptor cell death [14,31]. This resulted in a loss of retinal layer structure and marked retinal thinning, which was observed in a concentration-dependent manner after exposure to MNU [32]. We injected toxic substances and measured blood AST and ALT to determine liver toxicity in test animals. When MNU was provided, the AST increased by about 4-fold and ALT by about 2-fold or more. Severe hepatotoxicity was indicated by MNU, but the expressions of both biomarkers were significantly decreased when CA-HE50 was provided (**Fig. 6**). The eye tissue staining analysis confirmed the effects of MNU and CA-HE50 on tissue and changes in the cell layer. When MNU was provided, the arrangement of the ganglion cells layer (GCL) was disturbed, and the thicknesses of the outer plexiform layer (OPL) and outer nuclear layer (ONL) were significantly reduced. We identified retinal degeneration, including photoreceptor (inner and outer segments; IS and OS) and retinal pigment epithelium (RPE) destruction. However, when CA-HE50 was provided for 7 days and MNU was processed, the arrangement of the GCL was more regular than that of the MNU control, and the arrangement and thickness of the OPL and ONL were similar to normal control. CA-HE50 100 mg/kg appeared to indicate damage to the segment layer, but this observation may be due to the rolling phenomenon that occurs during the tissue sectioning. The arrangement of cells exposed to CA-HE50 200 mg/kg was uniform and the layer thickness was maintained similar to that of the normal control state, and the boundaries of each layer were clearly observed (**Fig. 7**).

Oxidative stress-induced damage in RPE cells results in changes such as apoptosis, mitochondrial DNA damage, increased expression of vascular endothelial growth factor (VEGF), decreased antioxidant enzymes, and increased inflammatory responses [33]. Biomarkers identified for these reactions include caspase-3 and PARP, which are involved in apoptosis [34,35], and NRF2, an antioxidant enzyme. To assess response to stress, HO-1, which functions in biological defense, was used to measure protein expression levels. The retinal epithelium has an antioxidant defense system controlled by NRF2. Studies of NRF2 in retinal epithelial layers have shown that this transcription factor plays an important role in protecting against oxidative problems derived from phototoxic stress [36]. HO-1 is also an important mediator of NRF2-induced protection, which acts through the signaling molecule carbon monoxide to produce the antioxidants biliverdin/bilirubin and to degrade heme [37]. Therefore, we measured the expressions of NRF2/HO-1 protein. As seen in **Fig. 8A**, the expression pattern of NRF2/HO-1 was the same and then decreased significantly in the presence of MNU and increased CA-HE50 in a concentration-dependent manner. Pro-PARP was expressed dose-dependently like the normal control level CA-HE50. The expression of pro-caspase 3 in the CA-HE50 200 mg/kg group was higher than that of normal control. However, we could not identify the cleavage forms of caspase-3 and PARP in this study. Therefore, it was difficult to directly evaluate whether the expressions of proforms were merely increased or whether they actually inhibited DNA fragmentation. Therefore, further studies of the inhibition of photoreceptor apoptosis by CA-HE50, AS, and AA are required to determine whether and which signaling pathways are related to cytoprotective effects (**Fig. 8A**). Rhodopsin, which is the combination of opsin and 11-cis-retinal, is an essential G-protein receptor in photo-transduction [38]. When the light comes into contact with light-sensitive rhodopsin, the molecules inside it change to an "activated" status, and the

signaling material binds to the active rhodopsin and changes its structure. In this way, the light continues to change and transmits a visual signal to the retina and from there to the brain [39]. When rhodopsin and opsin decrease, the visual signal is difficult to transmit, affecting vision. Since the retina is damaged by MNU, it was thought that the expressions of rhodopsin and opsin in ONL and photoreceptors might be affected. The expression levels of both were confirmed by western blot (**Fig. 8B**). The expressions of rhodopsin and opsin, which were sharply reduced by the administration of MNU, were not only suppressed by CA-HE50 provision, but the expressions of rhodopsin and opsin were even higher than those of normal control at 200 mg/kg. In addition to the effects of CA-HE50 on the protection or inhibition of oxidative stress and apoptosis, we examined factors affecting cell protection. Since glucose metabolism and energy production are major factors in general cell protection [40,41], the effects of CA-HE50 on glucose uptake in RPE cells were examined under normal conditions. We determined the effects of stimuli on glucose uptake in PRE cells of CA-HE50, and confirmed them by studies of AS and AA in CA-HE50 (**Fig. 5**). Therefore, we determined that CA-HE50 promotes glucose uptake in RPE cells, possibly due to the AS and AA present in CA-HE50.

In conclusion, CA-HE50 is effective for inhibiting or preventing photochemical damage and photoreceptor apoptosis, which cause age-related eye degeneration. AS may be useful as a major potency ingredient, and further analysis of the mechanisms underlying its effects should be studied. Although further, a more in-depth research is needed, we believe that there is enough evidence to develop drugs or dietary supplements for the treatment of age-related eye degeneration using CA-HE50.

REFERENCES

1. Niccoli T, Partridge L. Ageing as a risk factor for disease. Curr Biol 2012;22:R741-52.
   PUBMED | **CROSSREF**

2. Kumar V, Khan AA, Tripathi A, Dixit PK, Bajaj UK. Role of oxidative stress in various diseases: relevance of dietary antioxidants. J Phytopharm 2015;4:126-32.

3. Masuda T, Shimazawa M, Hara H. Retinal diseases associated with oxidative stress and the effects of a free radical scavenger (edaravone). Oxid Med Cell Longev 2017;2017:9208489.
   PUBMED | **CROSSREF**

4. Benedetto MM, Contin MA. Oxidative stress in retinal degeneration promoted by constant LED light. Front Cell Neurosci 2019;13:139.
   PUBMED | **CROSSREF**

5. Pan J, Kai G, Yuan C, Zhou B, Jin R, Yuan Y. Separation and determination of madecassic acid in triterpenic genins of Centella asiatica by high performance liquid chromatography using beta-cyclodextrin as mobile phase additive. Se Pu 2007;25:316-8.
   PUBMED | **CROSSREF**

6. Orhan IE. Centella asiatica (L.) urban: from traditional medicine to modern medicine with neuroprotective potential. Evid Based Complement Alternat Med 2012;2012:946259.
   PUBMED | **CROSSREF**

7. Somboonwong J, Kankaisre M, Tantisira B, Tantisira MH. Wound healing activities of different extracts of Centella asiatica in incision and burn wound models: an experimental animal study. BMC Complement Altern Med 2012;12:103.
   PUBMED | **CROSSREF**

8. Bevege L. Centella asiatica: a review. Aust J Med Herbal 2004;16:15-27.

9. Gray NE, Zweig JA, Caruso M, Martin MD, Zhu JY, Quinn JF, Soumyanath A. Centella asiatica increases hippocampal synaptic density and improves memory and executive function in aged mice. Brain Behav 2018;8:e01024.
   PUBMED | **CROSSREF**

10. Anand T, Mahadeva N, Phani KG, Farhath K. Antioxidant and DNA damage preventive properties of Centella asiatica (L) Urb. Pharmacogn J 2010;2:53-8.
    CROSSREF

11. G V, K SP, V L, Rajendra W. The antiepileptic effect of Centella asiatica on the activities of Na/K, Mg and Ca-ATPases in rat brain during pentylenetetrazol-induced epilepsy. Indian J Pharmacol 2010;42:82-6.
    PUBMED

12. Park JH, Choi JY, Son DJ, Park EK, Song MJ, Hellström M, Hong JT. Anti-inflammatory effect of titrated extract of Centella asiatica in phthalic anhydride-induced allergic dermatitis animal model. Int J Mol Sci 2017;18:E738.
    PUBMED | CROSSREF

13. Ceremuga TE, Valdivieso D, Kenner C, Lucia A, Lathrop K, Stailey O, Bailey H, Criss J, Linton J, Fried J, Taylor A, Padron G, Johnson AD. Evaluation of the anxiolytic and antidepressant effects of asiatic acid, a compound from Gotu kola or Centella asiatica, in the male Sprague Dawley rat. AANA J 2015;83:91-8.
    PUBMED

14. Maurer E, Tschopp M, Tappeiner C, Sallin P, Jazwinska A, Enzmann V. Methylnitrosourea (MNU)-induced retinal degeneration and regeneration in the zebrafish: histological and functional characteristics. J Vis Exp 2014;92:e51909.
    PUBMED | CROSSREF

15. Kitamoto S, Matsuyama R, Uematsu Y, Ogata K, Ota M, Yamada T, Miyata K, Funabashi H, Saito K. Optimal dose selection of N-methyl-N-nitrosourea for the rat comet assay to evaluate DNA damage in organs with different susceptibility to cytotoxicity. Mutat Res Genet Toxicol Environ Mutagen 2015;786-788:129-36.
    PUBMED | CROSSREF

16. Chen YY, Liu SL, Hu DP, Xing YQ, Shen Y. N -methyl- N -nitrosourea-induced retinal degeneration in mice. Exp Eye Res 2014;121:102-13.
    PUBMED | CROSSREF

17. Yamada K. Cobalt: its role in health and disease. Met Ions Life Sci 2013;13:295-320.
    PUBMED | CROSSREF

18. Caltana L, Merelli A, Lazarowski A, Brusco A. Neuronal and glial alterations due to focal cortical hypoxia induced by direct cobalt chloride (CoCl2) brain injection. Neurotox Res 2009;15:348-58.
    PUBMED | CROSSREF

19. Mou YH, Yang JY, Cui N, Wang JM, Hou Y, Song S, Wu CF. Effects of cobalt chloride on nitric oxide and cytokines/chemokines production in microglia. Int Immunopharmacol 2012;13:120-5.
    PUBMED | CROSSREF

20. Kuehn S, Hurst J, Rensinghoff F, Tsai T, Grauthoff S, Satgunarajah Y, Dick HB, Schnichels S, Joachim SC. Degenerative effects of cobalt-chloride treatment on neurons and microglia in a porcine retina organ culture model. Exp Eye Res 2017;155:107-20.
    PUBMED | CROSSREF

21. Grimm C, Willmann G. Hypoxia in the eye: a two-sided coin. High Alt Med Biol 2012;13:169-75.
    PUBMED | CROSSREF

22. König J, Ott C, Hugo M, Jung T, Bulteau AL, Grune T, Höhn A. Mitochondrial contribution to lipofuscin formation. Redox Biol 2017;11:673-81.
    PUBMED | CROSSREF

23. Rodolfo C, Campello S, Cecconi F. Mitophagy in neurodegenerative diseases. Neurochem Int 2018;117:156-66.
    PUBMED | CROSSREF

24. Rodgers KJ, Ford JL, Brunk UT. Heat shock proteins: keys to healthy ageing? Redox Rep 2009;14:147-53.
    PUBMED | CROSSREF

25. Firląg M, Kamaszewski M, Gaca K, Bałasińska B. Age-related changes in the central nervous system in selected domestic mammals and primates. Postepy Hig Med Dosw 2013;67:269-75.
    PUBMED | CROSSREF

26. Eldred GE, Katz ML. Fluorophores of the human retinal pigment epithelium: separation and spectral characterization. Exp Eye Res 1988;47:71-86.
    PUBMED | CROSSREF

27. Sparrow JR, Zhou J, Cai B. DNA is a target of the photodynamic effects elicited in A2E-laden RPE by blue-light illumination. Invest Ophthalmol Vis Sci 2003;44:2245-51.
    PUBMED | CROSSREF

28. Holz FG, Bellman C, Staudt S, Schütt F, Völcker HE. Fundus autofluorescence and development of geographic atrophy in age-related macular degeneration. Invest Ophthalmol Vis Sci 2001;42:1051-6.
    PUBMED

29. Tsubura A, Yuri T, Yoshizawa K, Uehara N, Takada H. Role of fatty acids in malignancy and visual impairment: epidemiological evidence and experimental studies. Histol Histopathol 2009;24:223-34.
   PUBMED

30. Nakajima M, Yuge K, Senzaki H, Shikata N, Miki H, Uyama M, Tsubura A. Photoreceptor apoptosis induced by a single systemic administration of N-methyl-N-nitrosourea in the rat retina. Am J Pathol 1996;148:631-41.
   PUBMED

31. Tsubura A, Yoshizawa K, Kuwata M, Uehara N. Animal models for retinitis pigmentosa induced by MNU; disease progression, mechanisms and therapeutic trials. Histol Histopathol 2010;25:933-44.
   PUBMED

32. Zulliger R, Lecaudé S, Eigeldinger-Berthou S, Wolf-Schnurrbusch UE, Enzmann V. Caspase-3-independent photoreceptor degeneration by N-methyl-N-nitrosourea (MNU) induces morphological and functional changes in the mouse retina. Graefes Arch Clin Exp Ophthalmol 2011;249:859-69.
   PUBMED | CROSSREF

33. Kaarniranta K, Pawlowska E, Szczepanska J, Jablkowska A, Blasiak J. Role of mitochondrial DNA damage in ROS-mediated pathogenesis of age-related macular degeneration (AMD). Int J Mol Sci 2019;20:2374.
   PUBMED | CROSSREF

34. Zhang C, Baffi J, Cousins SW, Csaky KG. Oxidant-induced cell death in retinal pigment epithelium cells mediated through the release of apoptosis-inducing factor. J Cell Sci 2003;116:1915-23.
   PUBMED | CROSSREF

35. Farrokh-Siar L, Rezai KA, Patel SC, van Seventer G, Ernest JT. Human fetal retinal pigment epithelium induced apoptosis of Jurkat T-cells involves caspase activation and PARP cleavage. Invest Ophthalmol Vis Sci 2002;43:2288.

36. Bellezza I. Oxidative stress in age-related macular degeneration: Nrf2 as therapeutic target. Front Pharmacol 2018;9:1280.
   PUBMED | CROSSREF

37. Choo YY, Lee S, Nguyen PH, Lee W, Woo MH, Min BS, Lee JH. Caffeoylglycolic acid methyl ester, a major constituent of sorghum, exhibits anti-inflammatory activity via the Nrf2/heme oxygenase-1 pathway. RSC Adv 2015;5:17786-96.
   CROSSREF

38. Palczewski K. G protein-coupled receptor rhodopsin. Annu Rev Biochem 2006;75:743-67.
   PUBMED | CROSSREF

39. Mannu GS. Retinal phototransduction. Neurosciences 2014;19:275-80.
   PUBMED

40. Zhao Y, Wieman HL, Jacobs SR, Rathmell JC. Mechanisms and methods in glucose metabolism and cell death. Methods Enzymol 2008;442:439-57.
   PUBMED | CROSSREF

41. Huang CY, Pai YC, Yu LC. Glucose-mediated cytoprotection in the gut epithelium under ischemic and hypoxic stress. Histol Histopathol 2017;32:543-50.
   PUBMED